

Article

Characterizing residual current circulation and its response mechanism to wind at a seasonal scale based on High Frequency radar data

Lei Ren^{1,2}, Lingna Yang¹, Guangwei Pan¹, Gang Zheng³, Qin Zhu⁴, Yaqi Wang¹, Zhenchang Zhu^{4,5*} and Michael Hartnett⁶

¹ Institute of Estuarine and Coastal Research, School of Ocean Engineering and Technology, Sun Yat-sen University, Zhuhai 519082, P. R. China; renlei7@mail.sysu.edu.cn; yangln7@mail2.sysu.edu.cn; pangw6@mail2.sysu.edu.cn; wangyq335@mail2.sysu.edu.cn

² Southern Marine Science and Engineering Guangdong Laboratory (Zhuhai), Zhuhai 519082, China

³ The State Key Laboratory of Satellite Ocean Environment Dynamics, Second Institute of Oceanography, Ministry of Natural Resources, Hangzhou, China;

⁴ Southern Marine Science and Engineering Guangdong Laboratory (Guangzhou), Guangzhou 511458 China; zhuqin@gmlab.ac.cn; zhenchang.zhu@gdut.edu.cn

⁵ Guangdong Provincial Key Laboratory of Water Quality Improvement and Ecological Restoration for Watersheds, Institute of Environmental and Ecological Engineering, Guangdong University of Technology, Guangzhou, 510006, China; zhenchang.zhu@gdut.edu.cn

⁶ National University of Ireland Galway, Galway, Ireland; michael.hartnett@nuigalway.ie

* Correspondence: zhenchang.zhu@gdut.edu.cn

Abstract: Characteristics of residual currents is an indicator for net transport of sediment, nutrients and pollutants, and the dilution and diffusion of soluble substances in coastal areas, yet their driving mechanisms remain poorly understood. Here, we studied the characteristics of surface residual currents along the west coast of Ireland Island and its response mechanism to wind at a seasonal scale, based on the continuous observation data of high frequency radar (HFR) for one year. Our analyses indicate that wind has significant effects on generating surface residual currents, with correlation coefficients of 0.6 - 0.8 between wind speeds and residual current speeds at both annual and seasonal scales. However, correlation between the direction of residual currents and the wind direction was not as significant as speeds, likely because the direction of residual currents was not only affected by sea surface wind, but also by land boundary conditions in research area. Moreover, the residual currents had a significant eastward flow trend identical to the wind direction at the maximum wind speed time, during which the effect of tide on residual currents was relatively weak. Additionally, comparison among wind fields, HFR surface flow fields and surface residual current fields reveals that wind is the dominant driver of the variation of surface flow fields and residual flow fields. These findings shed light on coastal ecological and environmental management, and can assist prevention and mitigation of marine disasters, by providing helpful information for improving the ability and accuracy of forecasting coastal currents.

Keywords: High Frequency Radar, residual currents, wind speed, surface flow field, seasonal scale

Citation: Lastname, F.; Lastname, F.; Lastname, F. Title. *Remote Sens.* **2021**, *13*, x. <https://doi.org/10.3390/xxxx>

Academic Editor: Firstname Lastname

Received: date

Accepted: date

Published: date

Publisher's Note: MDPI stays neutral with regard to jurisdictional claims in published maps and institutional affiliations.



Copyright: © 2021 by the authors. Submitted for possible open access publication under the terms and conditions of the Creative Commons Attribution (CC BY) license (<https://creativecommons.org/licenses/by/4.0/>).

1. Introduction

To meet economic development needs, human beings use marine space to carry out a series of construction, such as offshore airport, offshore sightseeing platform, offshore construction platform, island reef construction and so on [1]. These offshore engineering and structures not only meet their own design functions, but also bear various complex and severe ocean loads including ocean currents. The stability of marine engineering and

structures under the action of ocean currents is a complex dynamic response process. Investigation into the driving mechanism of ocean currents is not only an important scientific issue, but also a key practical issue to be solved in marine disaster prevention and mitigation.

Ocean currents are one of the most important parameters to describe the movement of sea water. Except for periodical tidal currents, others can be classified as residual currents. Residual currents refer to the remaining part of the total ocean currents after deducting periodic currents. Different from the periodic tidal currents, movement of residual currents is unidirectional. Thus, residual currents can move for a long distance along a certain direction [3]. Although magnitude of residual currents is not large, they are directly relative to the direction of sediment movement, net transport of nutrients and pollutants, the dilution and diffusion of soluble substances [4]. Analysis on residual currents is also an effective method to study coastal sediment movement and environmental protection engineering [5]. By analyzing the response of residual currents to wind in the study area, the diffusion of industrial wastewater, domestic wastewater and ship oil spill in seawater can be prevented and reasonably treated [6].

Studies have adopted different methods to analyze residual currents, depending on the abundance of data sources, for instance, the veering angles of wind-driven currents within the surface layer range from 0° to 45° to the right of the wind direction (northern hemisphere), and its magnitudes are 2-3% of the wind speed. So a wind map was introduced to present the fractional variance of surface currents by Kim, *et al.* [7]. Moreover, the transfer functions in summer and winter are presented, which is used to examine the seasonal variation in ocean surface currents response to the wind. Because eddy-topography interactions (topographic stress) are difficult to resolved with numerical models, a parameterization had been proposed by Holloway [8] based on the statistical mechanical equilibria tendencies (Neptune effect). Most of the studies mentioned above focus on long-term behavior of ocean currents, which were based on monthly or even seasonal mean data. By contrast, Callies, *et al.* [9] used daily meteorological data and currents data for principal component analysis to assess changes in the North Sea circulation.

Residual currents can be affected by many factors, including topography, wind field, runoff, non-linear factors of inshore tidal wave, uneven seawater density, sea surface tilt and other factors [10,11]. Previous studies found that residual currents circulation dynamic process is significantly affected by sea-air coupling [12]. Wind transfers energy into the ocean through multi-scale ocean motion, which is the main source of mechanical energy driving mixing in oceans [13]. Due to the consumption of momentum by viscous forces in sea water movement, wind has the greatest influence on surface currents, and weakens with the increase of water depth. Since the wind acts directly on the upper layers of the water column, residual currents generated by the wind are predominated surface processes. However, whether and how residual currents correlate with winds remains poorly understood.

In this study, we investigated the characteristics of surface residual currents along the west coast of Ireland Island and its response mechanism to wind at a seasonal scale, based on the continuous observation data of high frequency radar (HFR). HFR has been widely used to monitor surface currents for coastal areas around the world [15]. Specifically, we used currents data based on HFR and Butterworth filters to obtain residual surface currents, and subsequently variations in residual currents. We combined such data with the wind field data to analyze the driving effect of wind on residual current at a seasonal scale, as winds in the study area are relatively large and have significant seasonal characteristics [14].

The outline of this paper is as follows. Section 2 gives a brief description of the methodologies used in this study, HFR system, atmospheric data and computation of residual surface currents. Section 3 presents results of residual surface currents to wind and the influence of wind on residual currents, followed by discussion in Section 4. Section 5 presents main conclusions.

45
46
47
48
49
50
51
52
53
54
55
56
57
58
59
60
61
62
63
64
65
66
67
68
69
70
71
72
73
74
75
76
77
78
79
80
81
82
83
84
85
86
87
88
89
90
91
92
93
94
95
96
97
98

2. Methodologies

2.1. Study area

The study area is located on the west coast of Ireland island, as shown in Figure 1. This area prevails westerly winds and ocean currents movements are strongly affected by the North Atlantic Oscillation and frequent low pressure systems [16,17]. The bathymetry in the study area ranges from 0 to 140 m, and the nearshore isobaths are roughly parallel to the coastlines. Affected by Atlantic meteorological system, the averaged wind speed in January and June is approximately 11 m/s and 7 m/s, respectively [18]. This Atlantic wind condition has a significantly important impact on the size and direction of the local residual current in the region, and the surface residual current is controlled by wind forcing. Previous studies about hydrodynamic characteristics in this area are mainly based on numerical modelling, rarely observations over a large domain with fine temporal and spatial resolution were obtained and used. It is the first time that continuous observation of surface currents was monitored and residual currents were extracted.

Western Ireland is one of the regions with the high wind and wave energy in the world. In April 2021, the Irish National Electricity Supply Board (ESB) announced a detailed plan to immediately start the development of 1.4 GW offshore floating wind farm in this region, which will be one of the largest marine renewable energy projects in the world. After completion, Ireland will become an exporter of clean energy. This will make great social contributions to Ireland and Europe. Thus, study on hydrodynamics of this area will be of great importance for the planning, construction and operation stages of this project.

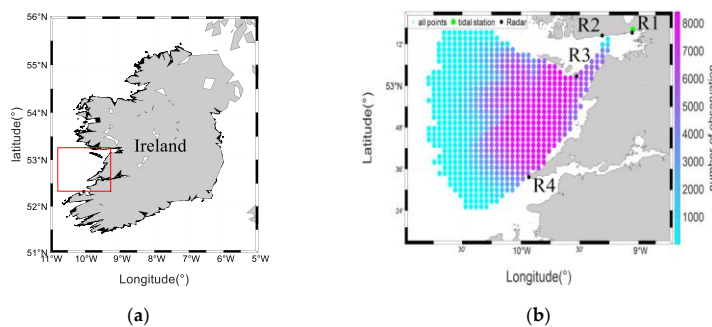


Figure 1. Study area and HFR coverage. (a) location of study area; (b) HFR coverage area and radar sites. (R1-R4 indicate the four HFR sites in the study area respectively)

Deployment location of HFR stations and its coverage area are shown in Figure 1(b). This study focuses on the analysis of sea surface currents observed by HFR system from a year's data, covering the offshore area with the maximum meridional and latitudinal length of approximately 100 km and 90 km separately (see Figure 1 (b)). In order to ensure reliability and integrity of the analyzed dataset, sea surface currents monitored for more than 80% of the observation period are defined as high density points, in total 162 points (see Figure 1 (b)). Surface currents at these pointed are selected for following analysis. The maximum latitudinal length and meridional length of high-density monitoring area are approximately 40 km and 50 km, respectively. Figure 1 (b) shows that majority of the high-density points are distributed in the intersection area between two HFR stations.

Wind data from an atmospheric model provided by European Centre for Medium-Range Weather Forecasts (ECMWF, <https://www.ecmwf.int/>). Detailed descriptions of each dataset are presented next.

99

100

101

102

103

104

105

106

107

108

109

110

111

112

113

114

115

116

117

118

119

120

121

122

123

124

125

126

127

128

129

130

131

132

133

134

135

136

137

Commented [HM1]: You will need to include references here to satisfy Reviewer

2.2. HFR system

HFR is an advanced type of remote sensing observation equipment, which has the advantages of large horizon, wide range and all-weather conditions [19]. HFR can extract sea state information such as wind field, wave field and flow field from radar echo [20,21]. Take flow field for example. Its observation principle is based on Bragg scattering [22]. The electromagnetic wave with wavelength λ emitted by HFR is incident on the ocean surface and propagates along the ocean surface. When encountering the ocean surface wave with wavelength $\lambda/2$ and the propagation direction of wave towards or away from HFR, the backscattering is the strongest, which is called Bragg scattering [23]. According to this principle, the echo spectrum can be obtained. The wave propagating towards radar produces positive spectrum peak, while the wave propagating away from radar produces negative spectrum peak [24]. This phenomenon is called Doppler frequency shift. In the case of surface current, the echo spectrum will generate a small frequency shift on the basis of the standard Doppler frequency shift. The radial currents velocity in the detection area can be obtained by inverting the small frequency shift through the corresponding relationship between the currents and the echo spectrum. The flow field data in the observation area can be obtained by superimposing the radial flow data measured by two or more HFR stations [16,25,26].

Since Crombie discovered the Bragg scattering in 1955, the research of HFR has been carried out rapidly based on it. After several research and development stages, it has been widely used in ocean remote sensing observation [27]. At present, the retrieval algorithm of currents velocity detected by HFR is relatively mature, which can obtain high-precision long-time series currents data and is suitable for the analysis of marine dynamic processes [28].

In this study, dataset was obtained from four HFR stations deployed by the National University of Ireland, Galway. In 2011, the portable Seasonde HFR stations R1 and R2 produced by Coastal Ocean Dynamics Application Radar (CODAR) company were deployed. Their operating frequencies are 26.425 MHz and 24.64 MHz, respectively, and their transmitted bandwidth is 499.88 KHz, range space is 0.3 km, velocity threshold is 150 cm/s, temporal resolution is 60 min and data averaging period is 94 min. The accuracy of HFR data is obtained by comparing the sea surface flow observed by HFR monitoring network of R1 and R2 stations with ADCP (Acoustic Doppler Current Profiler) data in the same region. Value of root mean square error (RMSE) is 10-12 cm/s, which proves the reliability of HFR observation data [29]. In 2014, other two HFR stations R3 and R4 were added in the west coast offshore area, and four stations were connected after that. Operating frequencies of R3 and R4 is 13.5 MHz, transmitted bandwidth is 49.63 KHz, range space is 3km, temporal resolution is 60 minutes and data averaging period is 75 minutes. Surface currents over a depth of approximately 1m from December 2015 to December 2016 monitored by HFR system were selected and used in this study. The HFR processing system preliminarily controls the data quality, and the maximum currents speed is set at 150 cm/s.

2.3. Atmospheric data

Since coastal surface currents are sensitive to wind conditions, in order to further investigate the relationship between wind and residual currents, wind data obtained from the European Centre for Medium-Range Weather Forecasts (ECMWF) at 0.125°×0.125° spatial resolution with 6 hours' temporal resolution were used.

To study wind variation characteristics during the analysis year, a wind rose of ECMWF data for 2016 is shown in Figure 2. In general, wind direction refers to the direction in which the wind blows from, and the direction of residual currents refer to the direction in which the residual currents flow to. In the subsequent rose diagram, the wind direction and the residual flow direction are plotted based on the same definition.

The variation a range of wind speeds is from 0.03 m/s to 21.96 m/s. The averaged wind speed is 7.28 m/s. Its dominant wind direction is southwest, accounting for approximately 40% of the whole year; while winds from northwest direction accounts for nearly one third of the whole year. It indicates that the wind direction in study area is mainly western, which is consistent with the fact that study area is located in the westerly belt [17].

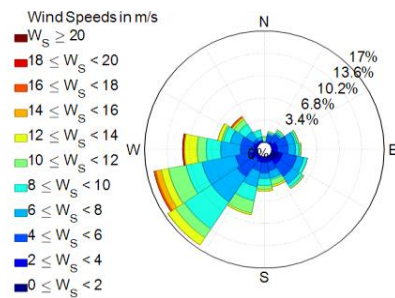


Figure 2. Wind rose for full year 2016.

2.4. Extraction of residual surface currents

In order to extract residual current data, a filtering technique is commonly used in physical oceanography to smooth and extract the time series, and to remove the fluctuation in the selected frequency band and change the signal phase. In this study, high frequency oscillation signals need to be filtered from the original HFR dataset.

There are a number of filters used in physical oceanography analysis such as Running-mean filters, Lanczos-window cosine filters, Kaiser-Bessel filters and Butterworth filters. Running-mean filters are the simplest, but its frequency response is poor in a relatively short dataset. Other filters mentioned above are more complex and precise. Lanczos-window cosine filters are simple and the filtering effect is better due to that the Lanczos window can reduce the leakage of redundant signals to the passband. When the filter parameter n is large enough, the Lanczos-window cosine filter has better ability to filter out the required information and suppress the interference information [30]. The Kaiser-Bessel filter is one of the best filters to process ocean data. It requires specification of a single parameter, and easy to generate coefficients with high equivalent noise bandwidth. Butterworth filters were used in this research considering the filtering effect and proficiency. This is a special type of recursive filter. Its transfer function is created by using rational functions in sine and cosine, and its output consists of input data and output past values. Different from the transfer function of the linear non-recursive filter constructed by truncated Fourier series, the transfer function of Butterworth filter is monotonically flat in the pass band and stop band, and has high tangency at the origin and Nyquist frequency [31]. Thus, Butterworth filter was selected and applied to extract residual surface currents.

In this research, raw surface currents data from a HFR system were filtered using the second-order Butterworth filter. The high-frequency signals (mainly the semidiurnal tide periodic signal represented by M2 and S2 tides) were filtered out, and the non-periodic characteristics (residual currents) contained in the raw data were retained. Through the comparison of filter threshold settings and filtering effects, the threshold value of the second-order Butterworth filter was set to 33 hours, filtering out the semidiurnal and diurnal

tide signals from raw HFR surface currents, and retaining the low-frequency residual currents signal [32]. The squared transfer function of the Butterworth low-pass filter can be expressed in the following formula [33]:

$$|H(\omega)|^2 = \frac{1}{1 + \left(\frac{\omega}{\omega_c}\right)^{2n}} = \frac{1}{1 + \varepsilon^2} \times \frac{1}{\left(\frac{\omega}{\omega_p}\right)^{2n}} \quad (1)$$

where n is the order of Butterworth low-pass filter, ω_c is the cut-off frequency, ω_p is the edge frequency, and $\frac{1}{(1+\varepsilon^2)}$ is the passband edge value of the low-pass filter. Values of ω_c and ω_p were set as 11.88kHz and 3.6kHz respectively in this research based on application by other studies.

3. Results

3.1. Response of residual surface currents to wind

To study the relationship between wind and residual surface currents, statistics of ECMWF wind speeds and HFR residual currents during the full analysis year and four seasons are computed and presented in Table 1.

Table 1. Statistics of wind speeds and HFR residual surface vector speeds.

Variable	Statistics	Spring	Summer	Autumn	Winter	Full Year
		(Mar.- May.)	(Jun.- Aug.)	(Sept.- Nov.)	(Dec.- Feb.)	
Wind Speed (m/s)	Maximum	21.31	14.28	18.26	21.96	21.96
	Average	6.64	6.38	7.21	9.03	7.28
	Minimum	0.14	0.13	0.03	0.42	0.03
Residual Current Speed (cm/s)	Maximum	25.12	27.17	35.65	41.18	41.18
	Average	10.12	9.86	12.36	16.28	11.8
	Minimum	0.63	0.2	0.25	0.31	0.16

Both wind speed and residual currents velocity display clear seasonal variation (Table 1). The maximum annual wind speed by 21.96 m/s and the maximum residual currents velocity by 41.18 cm/s occur in winter. In addition, the averaged wind speed (9.03 m/s) and averaged residual currents velocity (16.28 cm/s) are the largest in winter. The averaged values of wind speed and residual currents velocity are least in the summer; while the maximum residual currents velocity in spring is a minimum.

To explore the response mechanisms of residual surface currents to wind, rose diagram and vector diagrams of spatially averaged residual surface current vectors and wind vectors over the full analysis year are shown in Figure 3 and 4, respectively.

Commented [HM2]: Should you call this 'second-order transfer function' to be consistent with the comments from Reviewer #2?

Commented [HM3]: Can you provide a reference for these values

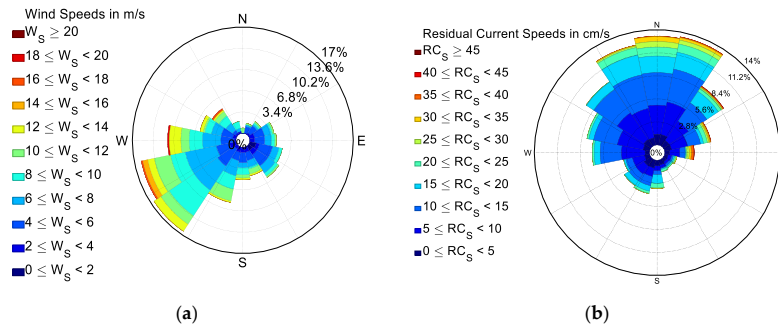


Figure 3. Rose diagrams for full year 2016 (a) wind; (b) residual currents.

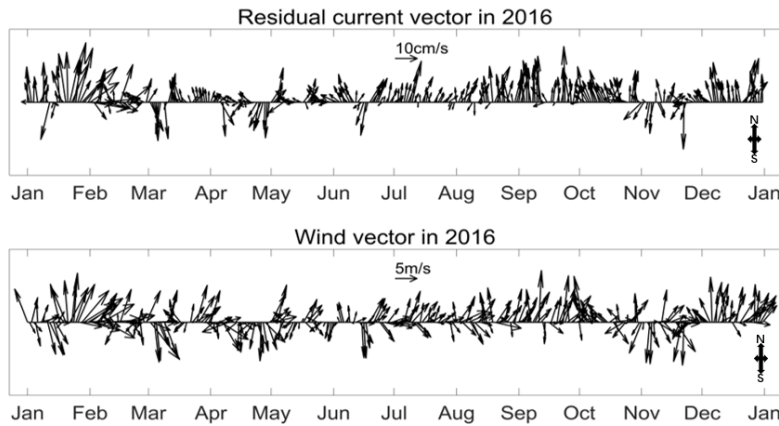


Figure 4. Vector time series of residual currents and winds during the analysis year.

Wind speed is between 0 and 22 m/s during the analysis period in the study area, and the residual currents velocity magnitude is between 0 and 42 cm/s. The dominant wind direction is southwest, accounting for approximately 40% of the whole analysis year; while the northwest wind direction accounts for approximately one third. This indicates that the wind is mainly westerly during the analysis period, this is consistent with geographic location of the study area. From the statistical analysis, correlation coefficients of zonal and meridional component between wind vectors and residual currents vectors over the analysis year are 0.76 and 0.68, respectively. This further indicates that residual surface currents in the study area are significantly affected by wind.

To further explore the influence of wind on coastal surface residual currents in different seasons, detailed correlation analyses between wind and residual currents in four seasons were carried out as detailed below.

254
255

256
257

258
259
260
261
262
263
264
265
266
267
268
269
270

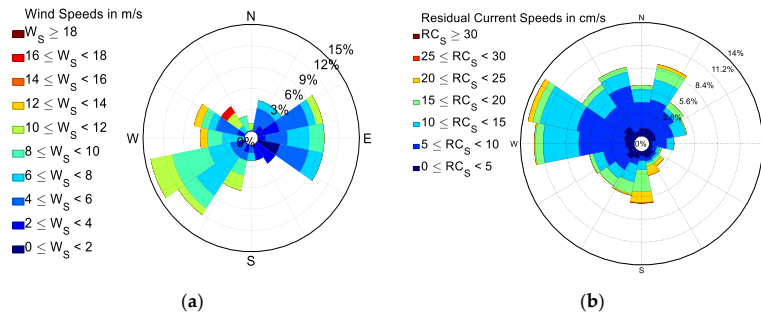


Figure 5. Rose diagram during spring. (a) wind; (b) residual currents.

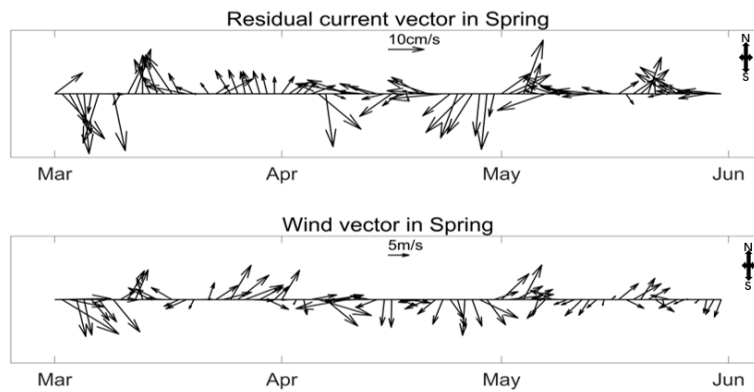


Figure 6. Vector time series of residual currents and winds in spring.

Wind speed in spring is between 0 and 22 m/s, and the residual currents velocity is between 0 and 26 cm/s. Figure 5 shows that the direction of residual currents is mainly west and northwest. While there is no obviously wind direction in the spring rose diagram among the wind directions, the directions of east and southwest take the larger proportion. Correlation coefficients of zonal and meridional component between wind speeds and residual currents speeds are 0.74 and 0.70, respectively. This indicates that wind is the main driving force generating residual surface currents. However, the directions of residual currents do not correlate well with the directions of wind. Because the study area is a coastal region with small scale (40 km×50 km), though the movements of residual currents are driven by wind force significantly according to the relative analysis, the residual currents directions are also influenced by the land mass in the study area. As shown in Figure 6 and Figure 5(b), the southerly wind is significant in spring. The southerly winds render the residual currents varying into westerly directions due to block of the land of west coast. This explains the difference between directions of wind and residual currents in Figure 5 and Figure 6. The vector time series in Figure 6 shows that the direction of residual currents has good agreement with the wind direction in spring according to the correlation analysis. Only in the middle of April and the middle of May, the residual currents vector shows a trend of northwest direction, while the wind vector shows a trend of southerly wind. This may be due to the effect of topography variation in a small scale (40 km×50 km) region [34].

271
272
273

274
275

Commented [HM4]: You need to address comment 4 by Reviewer #1 here - link between fig 1b and fig 6

276
277
278
279
280
281
282
283
284
285
286
287
288
289
290
291
292
293
294
295

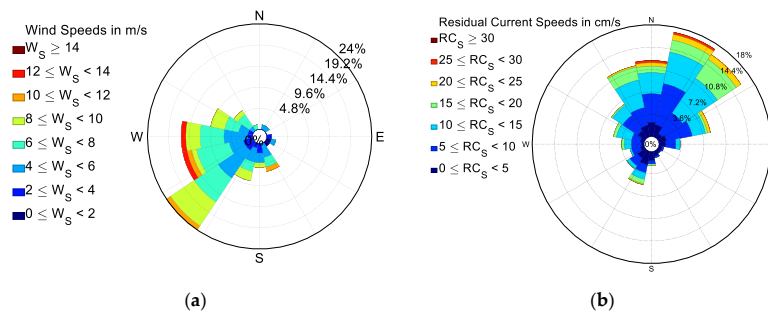


Figure 7. Rose diagram for summer. (a) wind; (b) residual currents.

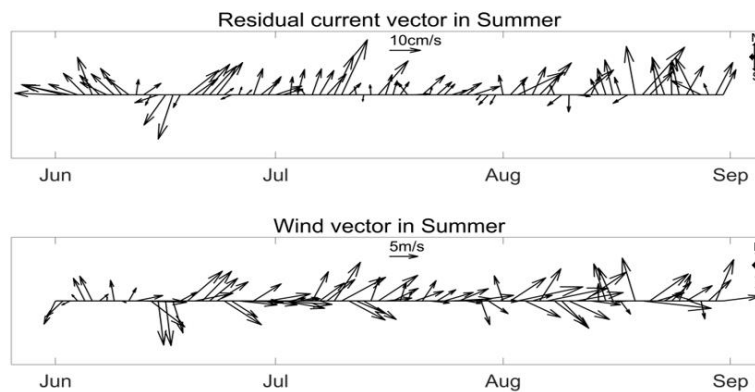


Figure 8. Vector time series of residual currents and winds in summer.

From Table 1, the averaged wind speed in summer is 6.38 m/s and the maximum wind speed in summer is 14.28 m/s, which are the minimum values in the statistics among four seasons and full year. As is shown in Figure 7, the main residual currents' direction is northeast while the wind direction is southwest. The direction of wind and residual currents qualitatively compare well. However, the difference between residual currents' direction and wind direction can be shown in the summer vector diagram, as shown in Figure 8. The averaged wind speed, the maximum wind speed, the averaged and maximum velocity of residual currents are the lowest of the four seasons. Good agreement exists between wind vectors and residual surface vectors when the wind speed is high, see Figure 8. Correlation coefficients of zonal and meridional components between residual currents vectors and wind vectors are lower in summer than in other seasons at 0.69 and 0.61, respectively. It shows that the direction of residual flows in summer had a significant difference when wind speeds are low. Fernand, Nolan, Raine, Chambers, Dye, White and Brown [18] indicated that currents speed and direction didn't correlate well except during the period with strong south-westerly winds. Therefore, the currents directions are not only driven by wind but also affected by the topography in the study area.

296

297

298

299

300

301

302

303

304

305

306

307

308

309

310

311

312

313

314

315

316

317

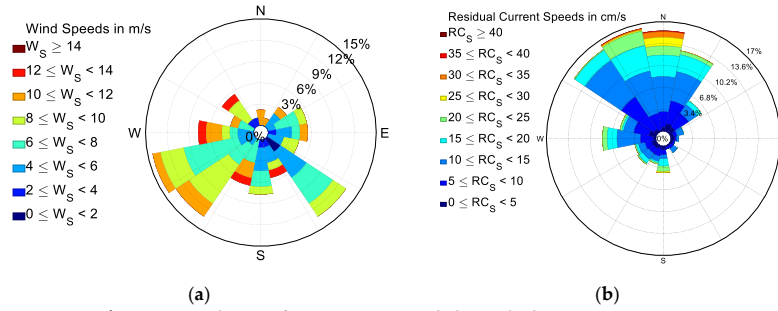


Figure 9. Rose diagram for autumn. (a) wind; (b) residual currents.

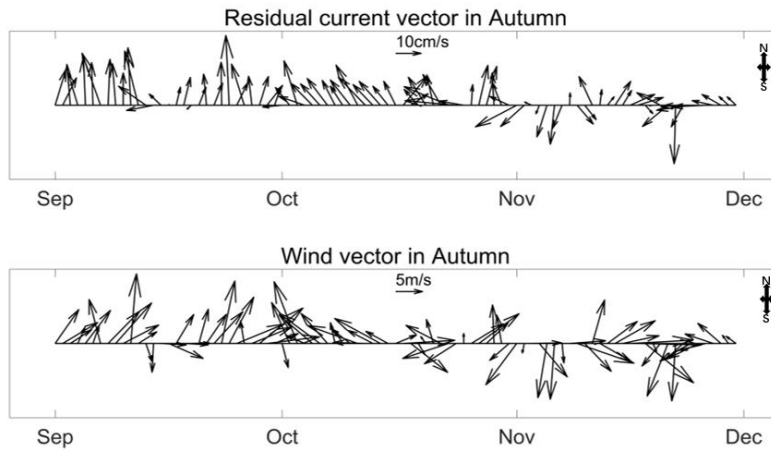


Figure 10. Vector time series of residual currents and winds in autumn.

Wind speed in autumn is between 0 and 19 m/s, and the residual currents velocity is between 0 and 36 cm/s. Averaged residual currents' velocity, the maximum residual currents' velocity, averaged wind speed and maximum wind speed of other currents are only lower than in winter. The direction of residual current flow in autumn is mainly from south to north, as is shown in Figure 9. Wind direction distribution in autumn is diverse, but southwest is still the dominant direction, followed by southeast. The correlation between wind speed and residual currents velocity in autumn is the highest, as is shown in Figure 10. Correlation coefficients of zonal and meridional components between residual currents vectors and wind vectors are 0.8 and 0.75, respectively. Statistically good agreement between wind direction and residual currents direction existed in autumn. This indicates that wind has a significant impact on driving residual current flow in autumn.

318
319
320

321
322
323
324
325
326
327
328
329
330
331
332
333
334

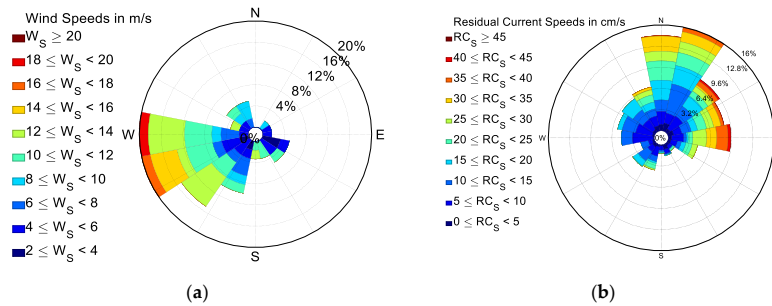


Figure 11. Rose diagram for winter. (a) wind; (b) residual currents.

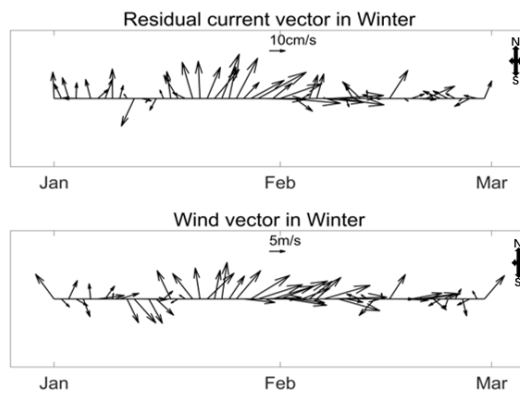


Figure 12. Vector time series of residual currents and winds in winter.

In winter, the wind speeds are between 0 and 22 m/s, the maximum wind speed occurs in this season; the residual currents velocities are between 0 and 42 cm/s, the maximum residual currents velocity occurs in this season. Figure 11 shows that the dominant flow direction in winter is northeast, followed by northwest. Northern flow trend is significant. Correlation coefficient of zonal and meridional components between residual currents vectors and wind vectors are 0.75 and 0.6 respectively. Figure 12 showed that direction of residual currents had a strong response to wind direction variation in winter except for in the first ten days in February when a northwest wind occurred.

3.2. Influence of the maximum wind on residual currents

To investigate the influence of regional wind fields on surface residual flow fields under extreme wind speed conditions at seasonal scale, wind vector fields, currents vector fields and residual currents vector fields corresponding to the maximum spatially-averaged wind speed (21.31 m/s, 14.28 m/s, 18.26 m/s, 21.96 m/s, see Figure 13) in the four seasons are analyzed. Through comparisons between wind fields and residual currents fields at time of the maximum wind speed during the four seasons, the effect of wind

335
336

337
338

339

340

341

342

343

344

345

346

347

348

349

350

351

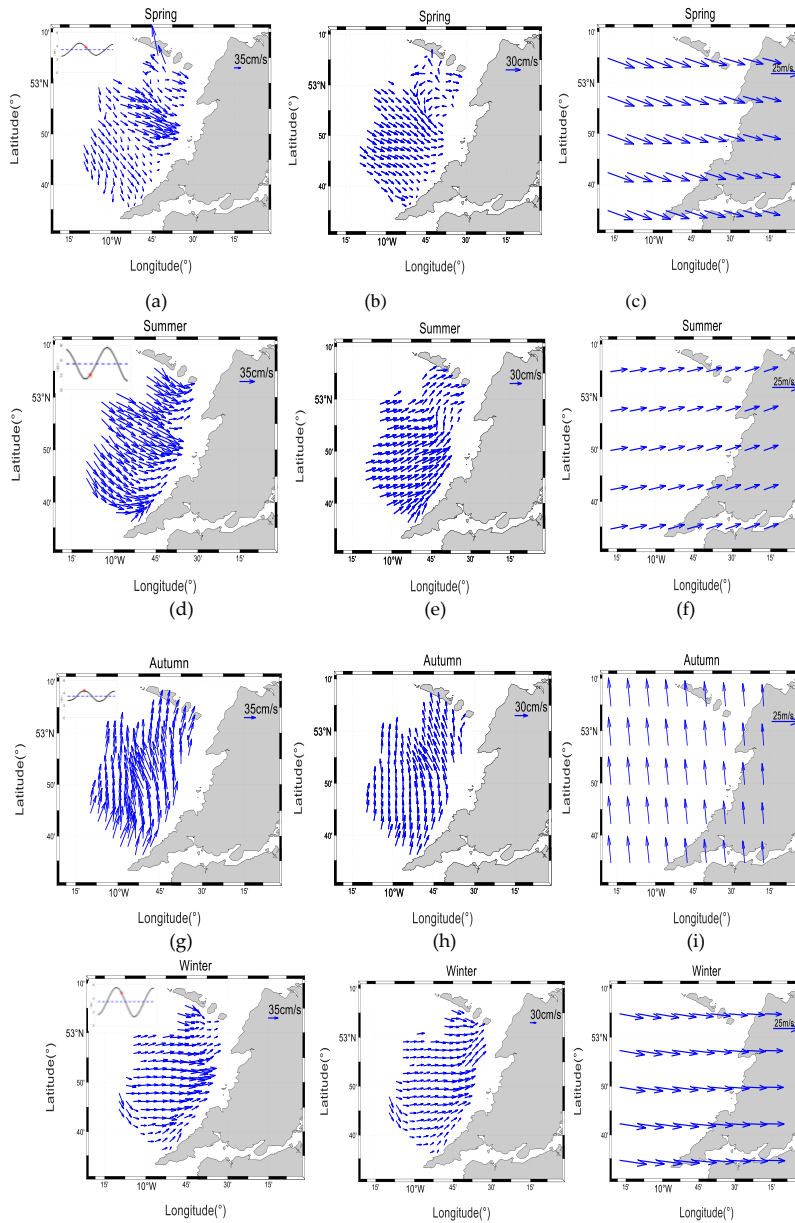
352

353

354

stress on the movement of residual currents is significant. At times corresponding to maximum spatially averaged wind speeds, residual current velocity is high; the strength of the wind field and the residual currents vector field have a high correlation.

355
356
357 **Commented [HM5]:** Reviewer #2 has a comment about this - can you address it?



(j) (k) (l)

Figure 13. Residual surface current vectors and HFR currents vector fields corresponding to the maximum atmospheric wind fields during four seasons. (a)(d)(g)(j) are original currents from HFR; (b)(e)(h)(k) are residual currents; (c)(f)(i)(l) are wind vectors. The panels at the top left of (a)(d)(g)(j) are the tidal phase corresponding to the maximum wind time (the red dot in the topleft subfigure is the tide level at the corresponding analysis time).

Figure 13 shows that the maximum wind speed in spring occurs in an ebbing tide, and the dominant wind direction are northwest (shore wind). At this time, the residual currents field presents an onshore flow tendency, which is not affected by the tidal force at this time. This reflects that the main driving factor of residual currents is wind stress, and tidal signals are well filtered after using the second order Butterworth method. At this time, the directions of the currents field and the residual currents field correlate well, showing a significant trend of onshore flow tendency, deeply affected by the wind stress and not reflecting the characteristics of the flow pattern in ebb tide period.

The maximum wind speed in summer is during a rising tide, and the dominant wind direction is southwest, consistent with the direction of tidal dynamics. The residual flow exhibits a strong onshore flow characteristic. At the same time, the dominant flow direction of the currents field is different from that of the residual currents field in the same period at some spatial points, but its trend is consistent overall, which shows the characteristics of onshore flow.

The maximum wind speed in autumn is at slack flood tide. The direction of the residual currents is mainly affected by a southerly wind, which exhibits a northward flow tendency. Onshore flows are not obviously presented during this period. The currents direction is consistent with that of the residual currents, showing a trend of northward flow.

In winter, the maximum wind speed is during an ebbing tide. The wind direction is westerly, which is uncorrelated with the direction of tidal dynamic propagation.

There is a significant correlation between the spatially-averaged residual currents vector direction and the spatially-averaged wind vector direction at the time of the maximum wind speeds. The corresponding relationship between the wind direction and the direction of residual currents from spring to autumn can be seen directly. For the maximum wind speed in winter, the wind direction and direction of residual currents present obvious characteristics of westerly and easterly, the movement of the residual currents and wind is mainly in the zonal velocity component, and their movement in the meridional velocity component is not obvious; therefore, the residual currents vector and wind vector at the maximum wind speed point in winter still correlates well.

Table 2. Statistics of the maximum wind for each season.

Variable	Statistics	Spring	Summer	Autumn	Winter
Wind	Maximum	25.68	16.05	21.19	27.1
Speed	Minimum	15.17	12.12	14.74	13.73
(m/s)	Average	21.32	14.32	18.26	21.98
Residual Surface	Maximum	22.26	36.82	38.83	73.26
Current Speed	Minimum	1.85	9.19	13.71	12.97
(cm/s)	Average	13.73	23.84	23.73	38.64
Surface	Maximum	66.65	41.44	62.89	100.24
Current Speed	Minimum	3.95	8.5	22.85	10.65
(cm/s)	Average	20.21	23.85	40.42	40.49

The wind speed range, as presented in Table 2, is from 12.12 m/s to 27.1 m/s at time of the maximum wind speed in each season, the range of residual currents vectors is from 1.85 cm/s to 73.26 cm/s, and instantaneous surface currents speed range of HFR is 3.95 cm/s to 100.24 cm/s. At the four times of the maximum wind speeds, the averaged speed of currents observed by HFR is greater than the corresponding residual currents' speed. Among them, the average value of currents velocity is 25% larger than that of residual currents velocity. The range of currents values measured by HFR is 34.84% larger than the range of residual currents values; the range of currents value is 96.29 cm/s and that of residual currents is 71.41 cm/s. The range and magnitude of residual currents velocity being smaller than those measured by HFR proves that the tide filtering process in this study is effective again. Table 2 further shows that the residual currents vector and currents vector at the time of the maximum wind speed are mainly driven by wind stress.

The dominant wind direction of the spatial wind field during the spring maximum wind speed is northwest, and the corresponding residual currents flow field's direction is northwest in a majority of the study area and east in the area near the island in the north. The residual currents direction in most of the study area shows southeast flows corresponding to the northwest wind.

The dominant wind direction of the wind field corresponding to the maximum spatially-averaged wind speed in summer is southwest, while the residual currents field shows a trend of northeast direction. The difference in the distribution of the residual currents in the northern part of the study area is due to the blocking of the northern islands, which shows a trend of northern flow.

The dominant wind direction of the wind field at the time point corresponding to the maximum spatially-averaged wind speed in autumn is south, while the residual currents field shows a trend of northward flow. The residual currents field corresponding to the maximum wind speed in autumn is different in the southern and northern part of the study area. The residual currents in the northern part of the study area is blocked by the northern island, showing a trend of flow to the northwest, while the residual currents in the southern part of the study area shows an obvious northward flow trend.

The dominant wind direction of the wind field at the time point corresponding to the maximum spatially-averaged wind speed in winter is westerly, while the residual currents in the northeast sea area shows the trend of northeast flow, and the residual currents in the southwest sea area shows the trend of southeast flow, and the residual currents in other sea areas shows the trend of east flow.

In conclusion, the wind fields and the residual currents vector fields corresponding to the maximum averaged wind speed in four different seasons exhibit a significant spatial consistency.

4. Discussion

In this research, the HFR surface currents over a continuous year are divided into four groups at a seasonal scale to discuss the response of surface residual currents to wind. Daily averaged wind vectors and residual currents vectors are compared for each analysis season. The same time series were used to compute correlation coefficients, but the hysteresis of residual currents response to wind is not considered. Xing, *et al.* [35] found that the lag of residual currents response to wind varies from several hours to more than ten hours. In the analysis at daily scale, it is possible to further improve the correlation between residual currents and wind by deeply analyzing the influence of the lag effect.

The veering angles of the wind-induced residual currents ranges from 0 to 45 degrees to the right of the wind direction in the northern hemisphere [7]. Because the study area is located in the coastal area, effects of topography and shoreline can not be ignored. Angle between -90° and 90° can be considered that the residual currents is caused by the wind

396
397
398
399
400
401
402
403
404
405
406
407
408
409
410
411
412
413
414
415
416
417
418
419
420
421
422
423
424
425
426
427
428
429
430
431
432
433
434
435
436
437
438
439
440
441
442
443
444
445
446

[11]. When discussing the drifting in the finite deep sea, except that it is necessary to introduce a hypothesis of limited depth, the other assumptions are the same as those in the infinite deep sea, the solution satisfying the boundary conditions can be expressed as [30]:

$$W = \frac{(1+i)\tau_y \operatorname{sh}(1+i)a\xi}{2aA_i\rho \operatorname{ch}(1+i)ah} \quad (2)$$

where complex velocity $W = u + iv$, complex press $\tau = \tau_z + i\tau_y$. It can be seen that the smaller the water depth, the smaller the right deflection angle of the velocity with the increase of depth. In the ocean with very shallow water depth, the drifting flows almost along the wind direction from the surface to the seabed. Considering the influence of topography and water depth, the residual flow driven by wind can be distinguished more accurately. Moreover, the corresponding relationship between wind speed and residual currents in the study area can be further improved.

Residual currents include tidal residual currents, wind ocean currents and density currents. The wind force in the study area is strong, but the effect of tidal currents can not be ignored. When a tidal wave is transmitted from the ocean to nearshore, non-linear effects are enhanced due to the shallower water depth, and tide induced residual currents will be generated [36]. In the follow-up research, researchers can further study the response of residual currents to wind during both spring and neap tides. In the neap tide period, there may be a stronger correlation between residual currents and wind, which will further advance the study of wind mechanisms of wind on residual currents. Although residual currents are mainly driven by wind forces in the study area, the direction of the residual currents is also influenced by the topography especially at the periods of low wind speeds. In order to study its profound mechanisms, analysis of the residual water level can be exerted to figure out how the topography of the study area makes a deflection between wind directions and residual currents directions through the difference of barotropic gradient made by the sea level fluctuation in further study. Prediction of currents in the study area is going to be exerted on further study using machine learning methods. Through the analysis of the mechanism of currents in the study area, the vital driven factors of the currents will be chosen as an input of prediction model and implement prediction of currents in the study area.

Additionally, hydrodynamics is an important power source for material transport in coastal areas, and suspended sediment transport is an important embodiment of hydrodynamic change process. Residual currents are a special non periodic form of ocean current. Its variation characteristics indicates the net transport and long-term transport of estuarine and coastal materials, and the change of residual current structure makes the mechanism of suspended sediment transport quite different on different temporal and spatial scales. Therefore, investigation into characteristics of residual current circulation and its response mechanism to winds at a seasonal scale is of great importance for exploring material transport in study area.

5. Conclusions

Analysis on characteristics of residual surface currents at the west coast of the Ireland Island was carried out based on one-year continuous observations monitored by the HFR system. The main conclusions are as follows.

(1) The correlation coefficient of annual and seasonal wind speed and surface residual currents velocity is 0.6-0.8, showing a relatively strong correlation between winds and residual surface currents.

(2) From the direction of residual currents field and the corresponding wind rose diagram, the corresponding relationship between residual currents direction and wind direction is not significant. This is because the area is at a small-scale (40 km×50 km), the residual currents are not only affected by the sea surface wind, but also affected by land boundary conditions in the east of the study area.

Commented [HM6]: You need to address comment from Reviewer #2

(3) The residual currents are affected by wind stress and presents the characteristics of eastward flow, and does not show the characteristics of onshore flow corresponding to the period of flood tide. At the time corresponding to the maximum wind speeds in four seasons, tidal force doesn't show significant effect on the distribution of currents and residual currents' direction. The surface currents and residual currents are mainly affected by wind force instead. At times of the maximum wind speed, wind stress is the main driving factor for both residual flow field and currents field.

In short, investigation into response of residual surface currents to wind was undertaken based on observation from HFR system on the west of Ireland island. These findings are useful for ecological environment protection and treatment. Correlation between wind and residual surface currents provides important information for developing soft computing forecasting models based on artificial intelligent, which will be carried out in future research.

Author Contributions: Formal analysis, G. P. L. Y and Z. Z, L. R; investigation, writing—original draft preparation, G. P. L. Y, G. Z, Z. Z and L. R; writing—review and editing, L. R, M. H; visualization, Q. Z, Y. W and G. P; supervision, M. H, L. R; funding acquisition, Z. Z, M. H and L. R. All authors have read and agreed to the published version of the manuscript.

Funding: This research was funded by the National Natural Science Foundation of China (NSFC), Grant No. 51909290 and 51909038; the Science and Technology Program of Guangzhou, China, Grant No. 201904010430; Guangdong Provincial Science and Technology Department Project, Grant No. 2020A1414010264. We would like to thank ECMWF for providing wind data and the Irish Marine Institute for providing the tidal data.

Conflicts of Interest: The authors declare no conflict of interest.

References

1. Kim, S.J.; Korgersaar, M.; Ahmadi, N.; Taimuri, G.; Kujala, P.; Hirdaris, S. The influence of fluid structure interaction modelling on the dynamic response of ships subject to collision and grounding. *Marine Structures* **2021**, *75*.
2. Chen, H.; Tang, T.; Ait-Ahmed, N.; Benbouzid, M.E.H.; Machmoum, M.; Zaim, M.E.-H. Attraction, Challenge and Current Status of Marine Current Energy. *IEEE Access* **2018**, *6*, 12665-12685.
3. Wang, B.; Hirose, N.; Moon, J.-H.; Yuan, D. Difference between the Lagrangian trajectories and Eulerian residual velocity fields in the southwestern Yellow Sea. *Ocean Dynamics* **2013**, *63*, 565-576.
4. *Physical Oceanography*. Shi, M.C., Ed.; Shandong Education Press: Jinan, 2005; Vol. 60-120.
5. Yang, J.; Ding, W.; Cui, J.; Guo, S.; Iop. Characteristical analysis of tidal and residual currents in the sea area around Tangshan international tourism island. In Proceedings of Asia Conference on Geological Research and Environmental Technology (GRET), Electr Network, 2021.
6. Liu, G.; Liu, Z.; Gao, H.; Gao, Z.; Feng, S. Simulation of the Lagrangian tide-induced residual velocity in a tide-dominated coastal system: a case study of Jiaozhou Bay, China. *Ocean Dynamics* **2012**, *62*, 1443-1456.
7. Kim, S.Y.; Cornuelle, B.D.; Terrill, E.J. Decomposing observations of high-frequency radar-derived surface currents by their forcing mechanisms: Locally wind-driven surface currents. *Journal of Geophysical Research-Oceans* **2010**, *115*.
8. Holloway, G. Systematic forcing of large-scale geophysical flows by eddy-topography interaction. *Journal of Fluid Mechanics* **1987**, *184*, 463-476.
9. Callies, U.; Gaslikova, L.; Kapitza, H.; Scharfe, M. German Bight residual current variability on a daily basis: principal components of multi-decadal barotropic simulations. *Geo-Marine Letters* **2017**, *37*, 151-162.
10. Cheng, P.; Valle-Levinson, A. Influence of Lateral Advection on Residual Currents in Microtidal Estuaries. *Journal of Physical Oceanography* **2009**, *39*, 3177-3190.

11. Dong, N.; Wang, G. Residual Current Analysis of the Yellow River Mouth Area in Bohai Gulf. *Journal of oceanography of Huanghai & Bohai Seas* **1997**, *64*-69. 545
12. Matte, P.; Secretan, Y.; Morin, J. Drivers of residual and tidal flow variability in the St. Lawrence fluvial estuary: Influence on tidal wave propagation. *Continental Shelf Research* **2019**, *174*, 158-173. 546
13. Kilbourne, B.F. *On the topic of oceanic variability near the Coriolis frequency; generation mechanisms, observations, and implications for interior mixing*; 2015; pp. 150 pp-150 pp. 547
14. Poul, H.M.; Backhaus, J.; Dehghani, A.; Huebner, U. Effect of subseabed salt domes on Tidal Residual currents in the Persian Gulf. *Journal of Geophysical Research-Oceans* **2016**, *121*, 3372-3380. 548
15. Bradbury, M.C.; Conley, D.C. Using Artificial Neural Networks for the Estimation of Subsurface Tidal Currents from High-Frequency Radar Surface Current Measurements. *Remote Sensing* **2021**, *13*. 549
16. Dobrynin, M.; Kleine, T.; Düsterhus, A.; Baehr, J. Skilful Seasonal Prediction of Ocean Surface Waves in the Atlantic Ocean. *Geophysical Research Letters* **2019**, *46*. 550
17. Gonzalez, P.L.M.; Brayshaw, D.J.; Zappa, G. The contribution of North Atlantic atmospheric circulation shifts to future wind speed projections for wind power over Europe. *Climate Dynamics* **2019**, *53*. 551
18. Fernand, L.; Nolan, G.D.; Raine, R.; Chambers, C.E.; Dye, S.R.; White, M.; Brown, J. The Irish coastal current: A seasonal jet-like circulation %J *Continental Shelf Research*. **2006**, *26*. 552
19. Gui, R.Z. Adaptively Selecting Working Frequency to Reduce Disturbances in High Frequency Radar. *Acta Physica Polonica A* **2011**, *119*, 473-478. 553
20. Basanez, A.; Perez-Munuzuri, V. HF Radars for Wave Energy Resource Assessment Offshore NW Spain. *Remote Sensing* **2021**, *13*. 554
21. Saviano, S.; Esposito, G.; Di Lemma, R.; de Ruggiero, P.; Zambianchi, E.; Pierini, S.; Falco, P.; Buonocore, B.; Cianelli, D.; Uttieri, M. Wind Direction Data from a Coastal HF Radar System in the Gulf of Naples (Central Mediterranean Sea). *Remote Sensing* **2021**, *13*. 555
22. Tseng, Y.-H.; Lu, C.-Y.; Zheng, Q.; Ho, C.-R. Characteristic Analysis of Sea Surface Currents around Taiwan Island from CODAR Observations. *Remote Sensing* **2021**, *13*. 556
23. Cosoli, S.; Mazzoldi, A.; Gacic, M. Validation of Surface Current Measurements in the Northern Adriatic Sea from High-Frequency Radars. *Journal of Atmospheric and Oceanic Technology* **2010**, *27*, 908-919. 557
24. Chen, Y.-R.; Paduan, J.D.; Cook, M.S.; Chuang, L.Z.-H.; Chung, Y.-J. Observations of Surface Currents and Tidal Variability Off of Northeastern Taiwan from Shore-Based High Frequency Radar. *Remote Sensing* **2021**, *13*. 558
25. An, Z. Study of Ocean Currents Detection with HF Ground Wave Over-the-Horizon Radar. Doctor, Xidian University, 2008. 559
26. Xiao, J. Research on Current Data Processing Method of High Frequency Surface Wave Radar. Master, Wuhan University, 2017. 560
27. Silva, M.T.; Huang, W.; Gill, E.W. Bistatic High-Frequency Radar Cross-Section of the Ocean Surface with Arbitrary Wave Heights. *Remote Sensing* **2020**, *12*. 561
28. Novi, L.; Raffa, F.; Serafino, F. Comparison of Measured Surface Currents from High Frequency (HF) and X-Band Radar in a Marine Protected Coastal Area of the Ligurian Sea: Toward an Integrated Monitoring System. *Remote Sensing* **2020**, *12*. 562
29. Lei, R.; Manman, W.; Huayang, C.; Zhan, H.; Qingshu, Y.; Hartnett, M. Characteristics of coastal currents based on High Frequency radar and ADCP observations in the Strait of Georgia. *IOP Conference Series: Earth and Environmental Science* **2018**, *189*, 052042 (052046 pp.)-052042 (052046 pp.). 563
30. Shibendu, M.; Rajib, K.; Durbadal, M. Direct digital fractional-order Butterworth filter design using constrained optimization. *AEU - International Journal of Electronics and Communications* **2021**, *128*. 564
31. Emery, W.J.; E, T.R. *Data Analysis Methods in Physical Oceanography*, 2 ed.; Elsevier Science: 2001. 565

-
32. Ma, J. Rotary spectrum estimation of ocean current vector time series and its application. *ACTA Oceanologica Sinica* **1986**, 671-677. 587
588
33. Chen, Y. Spatio-Temporal Characteristics and Influencing Factors of Current in Qinhuangdao Coastal Area. Master, Shanghai Ocean University, 2019. 589
590
34. Wang, H.; Wu, L.; Chai, H.; Xiao, Y.; Hsu, H.; Wang, Y. Characteristics of Marine Gravity Anomaly Reference Maps and Accuracy Analysis of Gravity Matching-Aided Navigation. *Sensors (Basel, Switzerland)* **2017**, *17*. 591
592
35. Xing, C.; Zhao, Q.; Cao, X.; Yang, Y.; Song, L. Seasonal variation of the coastal currents in the Northern Bohai Strait. *Marine Environmental Science* **2020**, *39*, 334-339. 593
594
36. Hickey, B.M.; Hamilton, P. A spin-up model as a diagnostic tool for interpretation of current and density measurements on the continental shelf of the pacific northwest. *Journal of Physical Oceanography* **1980**, *10*. 595
596
597